

p14^{ARF} Prevents Proliferation of Aneuploid Cells by Inducing p53-Dependent Apoptosis

LORENA VENEZIANO,¹ VIVIANA BARRA,¹ LAURA LENTINI,¹ SERGIO SPATAFORA,¹
AND ALDO DI LEONARDO^{1,2,*}

¹Department of Biological, Chemical and Pharmaceutical Sciences and Technologies, University of Palermo, Palermo, Italy

²Centro di OncoBiologia Sperimentale (COBS) via San Lorenzo Colli, Palermo, Italy

Weakening the Spindle Assembly Checkpoint by reduced expression of its components induces chromosome instability and aneuploidy that are hallmarks of cancer cells. The tumor suppressor p14^{ARF} is overexpressed in response to oncogenic stimuli to stabilize p53 halting cell progression. Previously, we found that lack or reduced expression of p14^{ARF} is involved in the maintenance of aneuploid cells in primary human cells, suggesting that it could be part of a pathway controlling their proliferation. To investigate this aspect further, p14^{ARF} was ectopically expressed in HCT116 cells after depletion of the Spindle Assembly Checkpoint MAD2 protein that was used as a trigger for aneuploidy. p14^{ARF} Re-expression reduced the number of aneuploid cells in MAD2 post-transcriptionally silenced cells. Also aberrant mitoses, frequently displayed in MAD2-depleted cells, were decreased when p14^{ARF} was expressed at the same time. In addition, p14^{ARF} ectopic expression in MAD2-depleted cells induced apoptosis associated with increased p53 protein levels. Conversely, p14^{ARF} ectopic expression did not induce apoptosis in HCT116 p53KO cells. Collectively, our results suggest that the tumor suppressor p14^{ARF} may have an important role in counteracting proliferation of aneuploid cells by activating p53-dependent apoptosis.

J. Cell. Physiol. 231: 336–344, 2016. © 2015 Wiley Periodicals, Inc.

The main function of mitosis is to ensure the fidelity of the segregation of one copy of each chromosome into daughter cells. The Spindle Assembly Checkpoint (SAC) is a surveillance system working in mitosis that ensures chromosomal stability by preventing anaphase onset until all sister chromatids are properly attached to the mitotic spindle (amphitelic attachment). The SAC is regulated by the Mitotic Checkpoint Complex (MCC), whose formation is induced by one or more unattached kinetochores. The MCC binds and inhibits the Anaphase-Promoting Complex/Cyclosome (APC/C) avoiding chromosome mis-segregation (Silva et al., 2011). Defective mitoses, caused by weakening the SAC, could promote aneuploidy characterized by numerical and structural changes of chromosomes that contribute to genomic instability, typical of many human tumors (Weaver and Cleveland, 2009; Thompson and Compton, 2011). However, it is not yet clearly established if aneuploidy is a cause of tumor initiation. The vision that aneuploidy is linked to tumorigenesis may be doubted by data showing that mutations of SAC components are lethal early in the embryonic development of mice (Holland and Cleveland, 2009). Moreover, some results suggested that aneuploidy can even have tumour suppressive effects at least under certain conditions (Weaver and Cleveland, 2007; Sussan et al., 2008).

Nevertheless, a weakened or aberrant SAC can promote cancer, and one example is congenital Chromosomal Instability (CIN) caused by the mutation of the SAC component BubR1, that generates the Mosaic Variegated Aneuploidy (MVA) disease associated with early cancer development (Hanks et al., 2004). In addition, human tumor cells HCT116 and Murine Embryonic Fibroblasts (MEFs) haploinsufficient for MAD2 exhibit the aneuploid phenotype that could promote cancer development (Michel et al., 2001), as well as mice that are heterozygous for Centromere Protein E (CENPE) exhibit whole chromosome aneuploidy associated with the increase of spontaneous tumors (Weaver and Cleveland, 2007).

Although aneuploidy could potentially increase the risk of neoplastic transformation, this seems to occur when it is associated with mutations in tumor suppressor genes.

Consistent with this hypothesis, aneuploidy caused by MAD2 haploinsufficiency has been shown to increase both the frequency and number of tumors in a p53[±] background (Holland and Cleveland, 2009). Additionally, it was shown that aneuploidy in near diploid HCT116 cells is associated with activation of the p38-p53-p21^{waf1} axis (Thompson and Compton, 2010). A p53-controlled pathway could also play an important role in contrast to aneuploidy, resulting from various cellular insults like an altered spindle checkpoint, thus preserving chromosomal stability.

Previously, we showed that aneuploidy caused by MAD2 haploinsufficiency activated a p53-dependent senescence pathway in IMR90 human fibroblasts to counteract aneuploidy deleterious effects (Lentini et al., 2012). On the contrary, aneuploidy promoted by MAD2 post-transcriptional silencing appeared to be well tolerated in MCF10A epithelial cells where the ARF gene coding for p14^{ARF} is deleted (Lentini et al., 2012). In addition, we showed that primary human fibroblasts (IMR90) perceived DNMT1 absence, that would result in DNA

Abbreviations: MAD2, Mitotic Arrest deficiency 2; SAC, Spindle Assembly Checkpoint; siRNA, Small Interfering RNA.

The Authors declare no conflicts of interest.

Contract grant sponsor: University of Palermo;
Contract grant number: FFR 2012-13, ATE-0255.

*Correspondence to: Aldo Di Leonardo, Department of Biological, Chemical and Pharmaceutical Sciences and Technologies, University of Palermo, Italy.
E-mail: aldo.dileonardo@unipa.it

Manuscript Received: 4 November 2014

Manuscript Accepted: 24 February 2015

Accepted manuscript online in Wiley Online Library

(wileyonlinelibrary.com): 8 March 2015.

DOI: 10.1002/jcp.24976

hypomethylation, as a stress signal that activated a p14ARF/p53 pathway inducing G1 arrest. When this pathway was not working, cells progressed incorrectly in the cell cycle with altered DNA methylation (hypomethylation) that affected chromosomal segregation thus resulting in aneuploidy (Barra et al., 2012). These results suggest a potential role of p14^{ARF} in promotion and/or maintenance of the tolerance to aneuploidy. To further investigate the putative role of p14^{ARF} dysfunction in aneuploid tolerance, we used as a system model near diploid HCT116 cells in which p14^{ARF} is not functional because of promoter hypermethylation and gene mutation (Burri et al., 2001). We expressed ectopically the ARF gene in these cells where depletion of MAD2 by RNAi triggered aneuploidy. Here, we show that p14^{ARF} ectopic expression induced p53-dependent apoptosis of aneuploid cells caused by MAD2 post-transcriptional silencing. Collectively, our results suggest a new role for p14^{ARF} to control proliferation of aneuploid cells.

Material And Methods

Cells and cell culture

Colon cancer cells HCT116 with MIN phenotype (near-diploid cells) and p53^{-/-} HCT116 cells (kindly provided by Dr. B. Vogelstein, John Hopkins University, Baltimore, MD) were cultured in D-MEM with 10% FBS (GIBCO, Invitrogen, Monza, Italy), 100 U/ml penicillin and 0.1 mg/ml streptomycin. Cells were cultured in a humidified atmosphere of 4% CO₂ in air at 37°C.

Cell viability

To assess cell viability HCT116 cells were transfected with the specific siRNA (siMAD2 and siMAD2 scramble) and the plasmids pcDNA3.1 (empty) and pcDNA3.1-p14 for 72 h, harvested by trypsinization and collected in a tube with 4 ml of phosphate buffered saline (PBS). Cell suspension (100 µl) were mixed with 100 µl of Trypan Blue (Sigma–Aldrich, Milan, Italy) and 10 µl were placed in a Burkert chamber for cell counting.

Cell transfection

Twenty-four hours after plating, cells were transfected with MAD2 siRNA n°1 (5'-AUACGGACUCACCUUUTT-3'), MAD2 siRNA n°2 (5'-AAGUGGUGAGGUCCUGGAATT-3') or with control MAD2 scramble siRNA (5'-CAGUCGCGUUJGCGACUGG-3') at a final concentration of 60 nM. After additionally five hours these cells were transfected with the pcDNA3.1 empty plasmid or harbouring the p14^{ARF} c-DNA (kindly provided by S. Gazzeri, University J. Fourier, La Tronche, France). The day of transfection the siRNA or the plasmid DNA and the transfection reagent (Lipofectamine 2000, Invitrogen, Monza, Italy) were diluted separately in Opti-MEM (Invitrogen, Monza, Italy) mixed gently and then incubated for 5 min at room temperature. After incubation the siRNA and the plasmid DNA were mixed gently with Lipofectamine 2000 (Invitrogen, Monza, Italy), allowed to sit 30 min at room temperature to allow complex formation, and added to the plates with 2 ml of Medium for 72 h.

Real time qRT-PCR

Primers to be used in Real-Time qRT-PCR experiments were designed with Primer Express software (Applied Biosystems, Monza, Italy) choosing amplicons of 70–100 bp. The selected sequences were tested against public databases (BLAST) to confirm the identity of the genes. Total RNA was extracted from cells by using the RNeasy Mini kit according to the manufacturer's instruction (Qiagen, Milan, Italy). RNA was reverse-transcribed in a final volume of 40 µl using the High Capacity c-DNA Archive kit (Applied Biosystems) for 10 min at

25°C and 2 h at 37°C. Real-Time qRT-PCR reaction was performed as previously described (Barra et al., 2012). Real-Time qRT-PCR was done in a final volume of 20 µl comprising 1 × Master Mix SYBR Green (Applied Biosystems) and 0.3 µM of forward and reverse primers for MAD2 (Fwd: 5'-GCCGAGTTTTTCTCATTGG-3'; Rev: 5'-CCGATTCTTCCCACTTTTCA-3').

Western Blotting

Protein concentration was measured using the Bio-Rad Protein Assay (Bio-Rad, Milan, Italy). Proteins (50 µg) were separated by 10% SDS-PAGE containing 0.1% SDS and transferred to Hybond-C nitrocellulose membranes (Amersham Life Science, Little Chalfont, England) by electroblotting. The membranes were sequentially incubated with primary antibodies against p53 (mouse, ab1101 Abcam, Cambridge, UK), p21^{waf1} (mouse, ab18209 Abcam, Cambridge, UK), MAD2 (goat, C19-Santa Cruz, Heidelberg, Germany), p14^{ARF} (goat, C18-Santa Cruz, Heidelberg, Germany) and HRP-conjugated mouse (ab6789, Abcam, Cambridge, UK), or goat (ab97110, Abcam, Cambridge, UK) as secondary antibodies. The target protein was detected with enhanced chemiluminescence Western blotting detection reagents (Pierce, Milan, Italy). Membranes were stained by Ponceau-Red to confirm equivalent loading of total protein in all lanes. We used antibody against β-tubulin (mouse, SIGMA, Milan, Italy, 1:10,000) to confirm proteins loading. The WB bands were quantified with "ImageLab" software (Bio-Rad, Milan, Italy).

Determination of ploidy

Cells were treated with 0.2 µg/ml colcemid (Demecolcine, Sigma–Aldrich, Milan, Italy) for 4 h. Cells were harvested by trypsinization, swollen in 75 mM KCl at 37°C, fixed with 3:1 methanol/acetic acid (v/v), and dropped onto clean, ice-cold glass microscope slides. The slides were air dried and stained with 3% GIEMSA in phosphate-buffered saline for 10 min. Chromosome numbers were evaluated by looking at 50 metaphases for each sample using a Zeiss Axioskop microscope under a 63× objective. The experiment was repeated twice. The statistical analysis was done by using the Student's t Test.

Immunofluorescence microscopy

To visualize β-tubulin cells were grown on rounded glass coverslips and then fixed with Ethanol/Acetic acid 95:5 for 10 min, permeabilized with 0.1% TritonX (Sigma–Aldrich, Milan, Italy) in PBS for 15 min and blocked with 0.1% Bovine Serum Albumin (BSA) for 30 min, both at room temperature. Coverslips were incubated with a mouse monoclonal antibody against β-tubulin mouse (1:200, Sigma–Aldrich, Milan, Italy) over-night at 4°C, followed by a goat anti-mouse IgG-FITC secondary antibody (Sigma–Aldrich, Milan, Italy, diluted 1:100 in PBS) for 1 h at 37°C. Nuclei were visualized with 1 µg/ml of 4',6-Diamidino-2-phenylindole (DAPI) and examined on a Zeiss Axioskop microscope equipped for fluorescence, images were captured with a CCD digital camera (AxioCam, Zeiss, Milan, Italy) and then transferred to Adobe PhotoShop for printing. We evaluated at least 100 mitoses for each sample. The experiment was repeated twice.

Senescence-associated β-galactosidase activity assay

Senescence-Associated βGalactosidase (SA-βGal) activity was measured 72 h after siMAD2 RNA transfection, cells were washed in PBS, fixed for 3 min (room temperature) in 2% paraformaldehyde, washed, and incubated for 24 h at 37°C (no CO₂) with fresh SA-βGal stain solution: 1 mg/ml 5-bromo-4-chloro-3-indyl-D-galactopyranoside (X-Gal, SIGMA),

5 mmol/L potassium ferrocyanide, 5 mmol/L potassium ferricyanide, 150 mmol/L NaCl, 2 mmol/L MgCl₂, 0.01% sodium deoxycholate, and 0.02% Nonidet-40 (Lentini et al., 2012). Senescent cells were evaluated using a Zeiss Axioskop microscope under a 20× objective (100 cells/sample). The experiment was repeated twice.

Acridine orange/ethidium bromide assay

Acridine orange (AO) permeates all cells and makes the nuclei to appear green. Ethidium bromide (EB) is only taken up by cells when cytoplasmic membrane integrity is lost and stains the nucleus in red. Thus, live cells have a normal green nucleus, apoptotic cells have bright green nucleus with condensed or fragmented chromatin; cells died from direct necrosis have a structurally normal orange–red nucleus. Floating cells were collected in a 15 ml tube, adherent cells were harvested by trypsinization and added to the same 15 ml tube. Cells were centrifuged and resuspended in AO/EB solution then dropped onto glass microscope slides. Apoptotic cells were evaluated by using a Zeiss Axioskop microscope with a 20× objective. At least 150 cells for each sample were scored and the experiment was repeated twice.

Statistical analysis

All experiments were repeated at least twice and statistically analyzed by the Student's *t* Test. In the figures the symbol ** indicates a *P* value <0.01 and the symbol * indicates a *P* value <0.05.

Results

Ectopic expression of p14^{ARF} in MAD2 post-transcriptional silenced HCT116 cells induced slowing down of proliferation

Previously, we showed that post-transcriptional silencing of the MAD2 gene in primary human fibroblast (IMR90), mimicking MAD2 haploinsufficiency, induced aneuploidy followed by the increase of p14^{ARF} protein and premature cellular senescence. On the contrary, MCF10A cells that have the p14^{ARF} deleted did not activate a senescence pathway, though they became aneuploid after MAD2 post-transcriptional silencing. These results suggested a role for p14^{ARF} in aneuploidy control (Lentini et al., 2012). Accordingly, to understand if p14^{ARF} is able to counteract aneuploidy caused by MAD2 haploinsufficiency, we

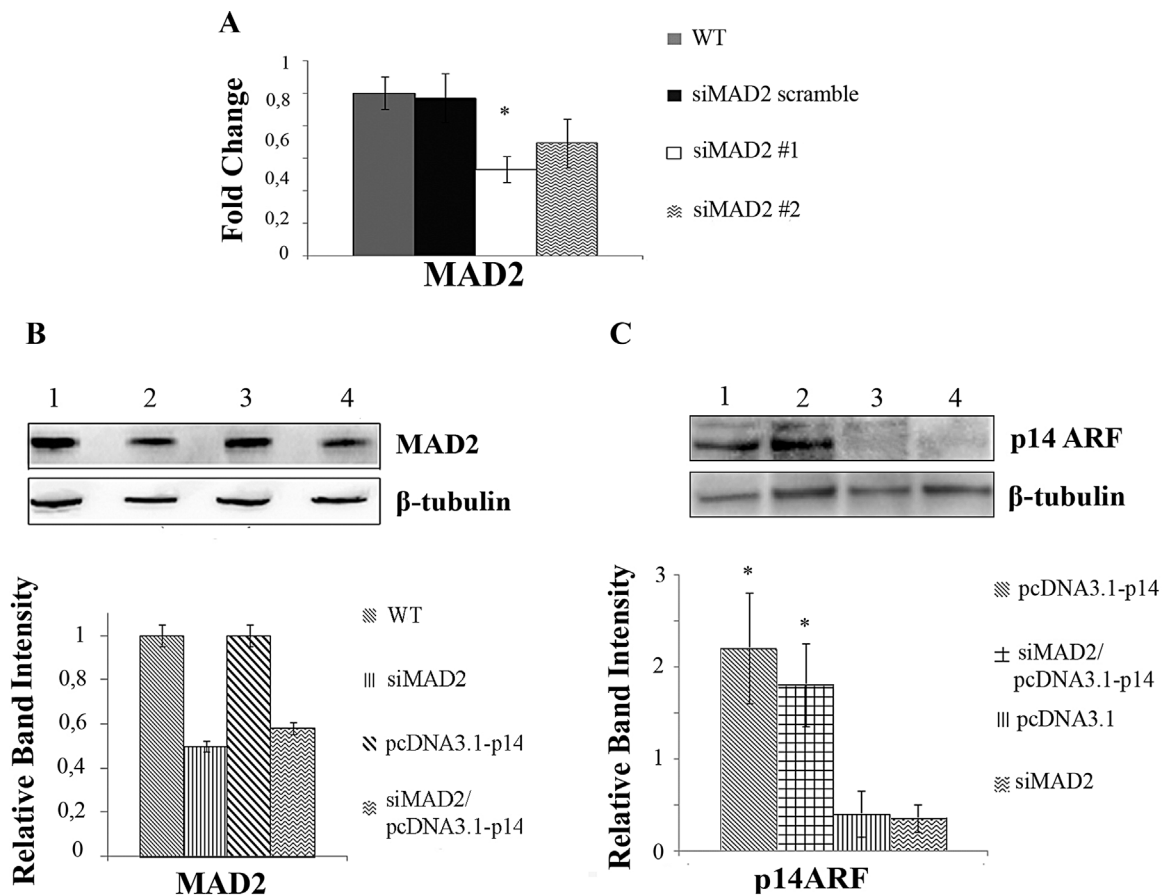


Fig. 1. p14^{ARF} ectopic expression and MAD2 post-transcriptional silencing in HCT116 cells. **A:** Real Time RT-PCR analysis showing RNA interference of siMAD2 #2, siMAD2 #1 and siMAD2-scramble at 72 h after transfection. **B:** Western Blot analysis at 72 h post transfection showing that RNA interference induced the reduction of MAD2 protein level in siMAD2 (2) and siMAD2/pcDNA3.1-p14 (4) HCT116 cells in comparison to WT (1) and pcDNA3.1-p14 (3) HCT116 cells, below the WB panel is showed the densitometry analysis to quantitate the MAD2 protein as normalized to β-Tubulin. **C:** Western blot analysis confirmed p14^{ARF} protein increase 72 h after pcDNA3.1-p14 plasmid transient transfection in HCT116 pcDNA3.1-p14 (1) and HCT116 siMAD2/pcDNA3.1-p14 (2) compared to HCT116 pcDNA3.1 (3) and HCT116 siMAD2 (4); the graph above shows p14^{ARF} protein levels normalized to β-Tubulin.

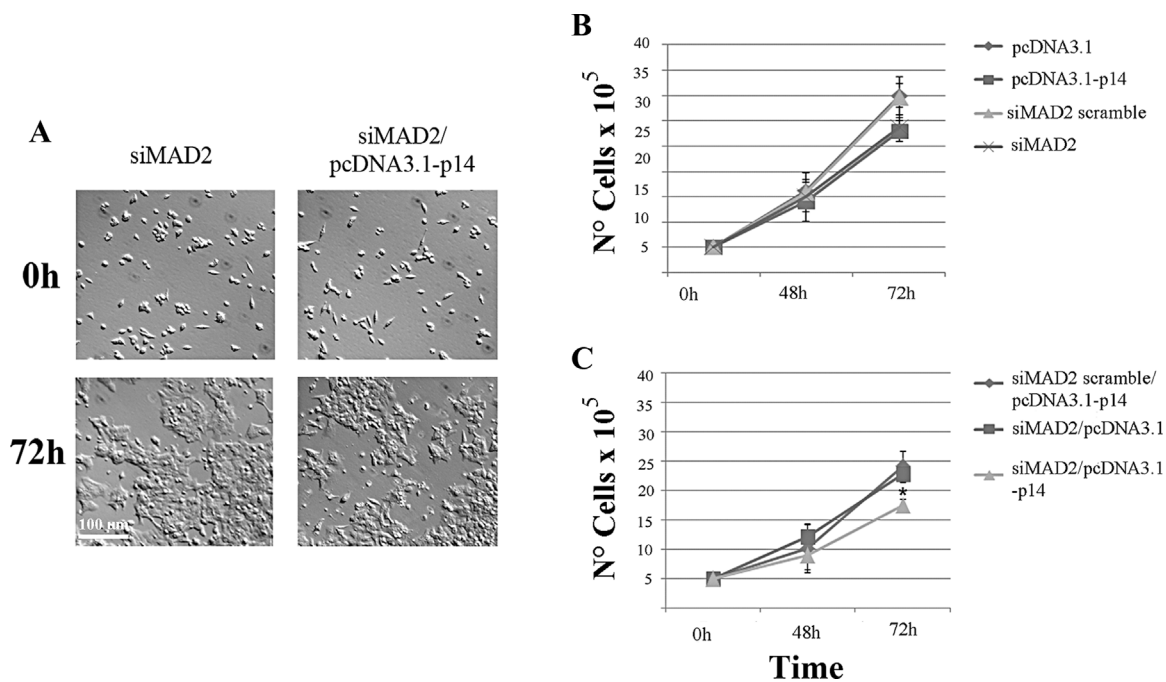


Fig. 2. p14^{ARF} ectopic expression reduces proliferation of MAD2-depleted HCT116 cells. **A:** Pictures showing the cell density/dish of siMAD2 and siMAD2/pcDNA3.1-p14 HCT116 cells at 0 and 72 h. **B:** The graph shows HCT116 cell proliferation at 0, 48, and 72 h after transfection of siRNA targeting MAD2 transcript (siMAD2), scrambled-siMAD2, and pcDNA3.1, pcDNA3.1-p14. **C:** The graph shows cell proliferation of siMAD2/pcDNA3.1, siMAD2/pcDNA3.1-p14, and siMAD2 scramble/pcDNA3.1-p14 HCT116 cells at 0, 48, and 72 h post transfection. The experiment was repeated twice. (Student's t test * $P < 0.05$; ** $P < 0.01$, $n = 50$).

ectopically expressed p14^{ARF} in HCT116 cells that have one p14^{ARF} allele deleted and the other allele is silenced by DNA hypermethylation of the promoter (Burri et al., 2001). HCT116 cells were chosen because they are an established near-diploid cell line that maintains a stable karyotype (Lengauer et al., 1997). In order to mimic MAD2 haploinsufficiency, we utilized the RNA interference strategy by using two different small interfering RNA (siRNAs) targeting the MAD2 transcript (siMAD2 #1, siMAD2 #2). Real-time qRT-PCR analysis showed that the siMAD2 #1 was able to reduce the amount of MAD2 transcript just about 50%. Thus, we decided to conduct all subsequent experiments using the siMAD2#1 (Fig. 1A). Western blot experiments confirmed that RNA interference reduced to about 50% the MAD2 protein in HCT116 transfected cells (Fig. 1B).

To express ectopically p14^{ARF}, HCT116 cells were transfected with the plasmid pcDNA3.1 carrying the p14^{ARF} c-DNA (Ayrault et al., 2006). By Western blot analysis, the p14^{ARF} expression was confirmed in all samples transfected with the pcDNA3.1-p14 plasmid when compared to HCT116-wt cells. Early effects of p14^{ARF} ectopic expression and MAD2 depletion were estimated by evaluating the cellular density/dish 48 h and 72 h post-transfection. While there were no statistically significant differences in proliferation between cells transfected with siMAD2 and siMAD2-scramble siRNAs, ectopic expression of p14^{ARF} induced a decrease of cell number in MAD2 silenced cells, as displayed by microscopic observation (Fig. 2A). This result seems to be caused by p14^{ARF} ectopic expression, since cells transfected with control cells (siMAD2 scramble/pcDNA3.1-p14 or siMAD2/pcDNA3.1) did not show

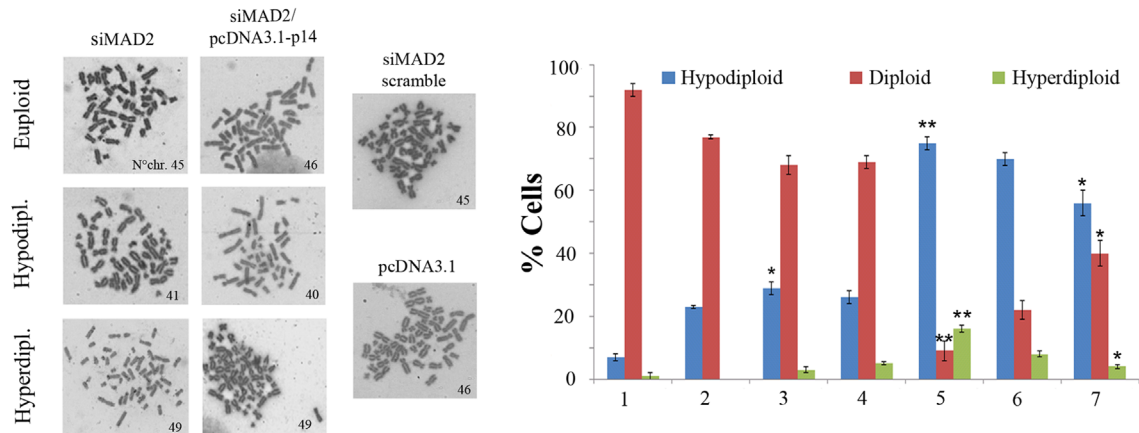
reduction in cell numbers at 72 h post transfection (Fig. 2B and C).

Ectopic expression of p14^{ARF} reduced aneuploid cells and mitotic abnormalities caused by MAD2 depletion

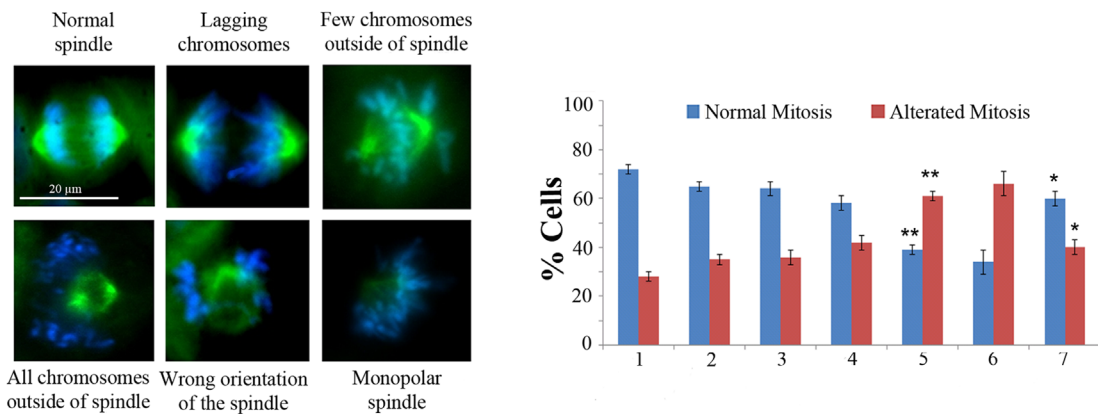
In agreement with previous reports (Thompson and Compton, 2010; Lentini et al., 2012) analysis of mitotic cells by cytogenetics revealed the presence of more than 90% of aneuploid cells after partial depletion of MAD2. The majority (75%) of these mitotic cells were hypodiploid and only 16% were hyperdiploid (Fig. 3A). Thus, weakening the SAC by MAD2 depletion induced aneuploidy in near diploid HCT116 cells. Previously, it was suggested that p14^{ARF} could play some roles in aneuploidy (Barra et al., 2012; Silk et al., 2013). To get additional clues on this aspect we estimated aneuploidy in HCT116 cells depleted of MAD2 and with transient expression of ectopic p14^{ARF}. Both in siMAD2-scramble and in pcDNA3.1-p14 HCT116 cells the aneuploidy level changed slightly in comparison to control. As expected the number of aneuploid cells dropped to 60% (56% hypodiploid and 4% hyperdiploid) after transient expression of ectopic p14^{ARF} in MAD2-depleted HCT116 cells. On the contrary, MAD2-depleted HCT116 cells and then transfected with the pcDNA3.1-empty vector still showed a high percentage of aneuploid cells (79%) similar to that shown by cells transfected with siMAD2 alone (Fig. 3A).

Since aneuploidy may be associated with aberrant mitosis, we then evaluated the presence of mitotic spindle alterations after p14^{ARF} ectopic expression and MAD2 depletion in HCT116 cells. Detection of β -tubulin of cells in mitosis

A



B



C

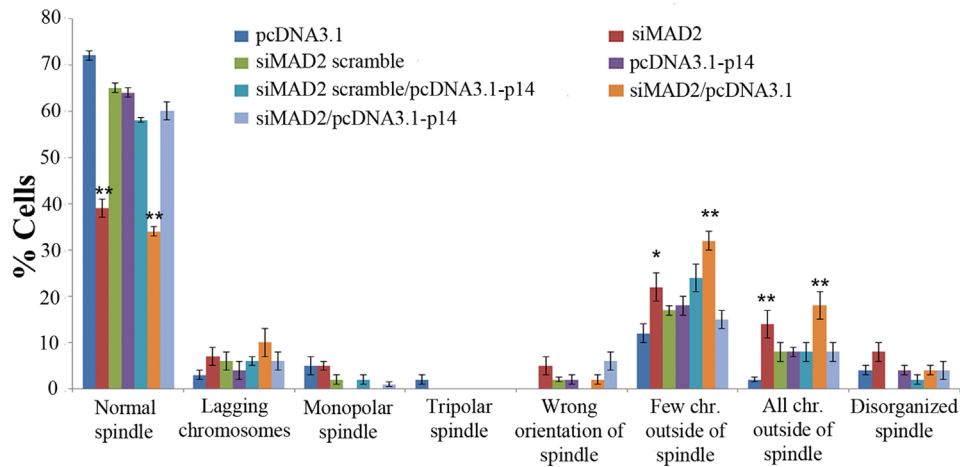


Fig. 3. Aneuploidy and mitotic alteration are reduced in HCT116 siMAD2 cells following p14^{ARF} ectopic expression. **A:** Representative pictures of aneuploid metaphases (left) found in siMAD2, siMAD2/pcDNA3.1-p14 HCT116 cells and euploid metaphases of pcDNA3.1, and siMAD2-scramble HCT116 cells (right). On the right the graph showing the percentages of aneuploid cells in HCT116 pcDNA3.1 (1) (Mitotic Index (MI):15), siMAD2-scramble (2) (MI:14), pcDNA3.1-p14 (3) (MI:13), siMAD2-scramble/pcDNA3.1-p14 (4) (MI:13), siMAD2 (5) (MI:6), siMAD2/pcDNA3.1 (6) (MI:11), and siMAD2/pcDNA3.1-p14 (7) (MI:9). **B:** On the right representative images of mitotic alterations detected by β -tubulin staining in all samples analyzed (DNA was stained with DAPI); on the left the percentages of normal and altered metaphases in pcDNA3.1 (1), siMAD2-scramble (2), pcDNA3.1-p14 (3), siMAD2-scramble/pcDNA-p14 (4), siMAD2 (5), siMAD2/pcDNA3.1 (6), and siMAD2/pcDNA3.1-p14 (7) HCT116 cells. **C:** The graph summarizes the percentages of specific mitotic spindle alterations detected. All experiments were repeated at least twice. (Student's t test * $P < 0.05$; ** $P < 0.01$, $n = 50$ metaphases).

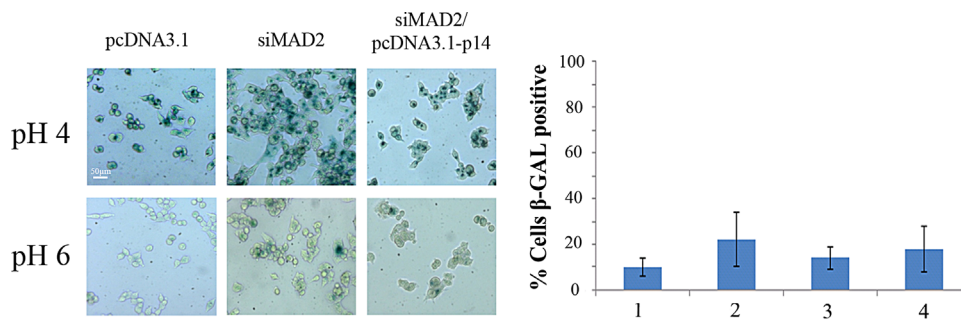


Fig. 4. p14^{ARF} does not induce cellular senescence in MAD2-depleted cells. On the left representative pictures of pcDNA3.1, siMAD2, and/or pcDNA3.1-p14 HCT116 cells, 72 h after transfection stained for β -gal (pH4: young and senescent cells, pH6: senescent cells). On the right the graph summarizes the percentage of senescent HCT116 cells (β -gal positive): pcDNA3.1 (1), siMAD2 (2), pcDNA3.1-p14 (3), and siMAD2/pcDNA3.1-p14 (4). The differences are not statistical significant.

revealed mitotic alterations as follows: monopolar spindles, all few chromosome outside of the spindle, and wrong orientation of the spindle. These altered mitosis were especially found in MAD2-depleted HCT116 cells (61%), and were reduced (40%) when p14^{ARF} was ectopically expressed (Fig. 3 B and C). These results are similar to those reported by the Weaver group where haploinsufficiency of CENPE, another player of the SAC, induced mitotic spindle alterations (Silk et al., 2013).

The finding that the percentage of altered metaphases is reduced in cells re-expressing p14^{ARF} in comparison to HCT116 siMAD2/pcDNA3.1, suggested that p14^{ARF} re-expression promotes the elimination of aneuploid cells caused by MAD2 depletion (Fig. 3 B and C).

p14^{ARF} ectopic expression induces apoptosis and not premature cellular senescence in aneuploid cells

Previously, we showed that post-transcriptional silencing of MAD2 and DNMT1 genes induced aneuploidy in human primary fibroblasts followed by premature cellular senescence, mediated by p14^{ARF}, as a possible way to block aneuploid cells (Barra et al., 2012; Lentini et al., 2012). We investigated then whether p14^{ARF} could activate the senescence pathway after MAD2 depletion in HCT116 cells. To this aim we conducted a senescence-associated β -galactosidase (β -gal) activity assay to evaluate the percentages of senescent cells after siMAD2 and p14^{ARF} ectopic expression. This assay was carried out at two different pH values: at pH6 only senescent cells were stained in blue while at pH4, that we used as a control, both senescent cells and proliferative cells were stained in blue. We found low percentages of β -gal positive cells in all samples analyzed (Fig. 4), suggesting that in MAD2-depleted HCT116 cells ectopic expression of p14^{ARF} does not activate a cellular senescence pathway.

Following simultaneous p14^{ARF} ectopic expression and siMAD2 post-transcriptional silencing, we found the presence of many floating cells (data not shown). To assess if apoptosis was responsible for these dead cells, we conducted the Acridine Orange/Ethidium Bromide (AO/EB) assay that distinguishes live cells from both apoptotic and necrotic cells (Fig. 5A). We found a high percentage of apoptotic (36%) and necrotic cells (17%) following p14^{ARF} ectopic expression and MAD2 depletion. By applying the Student's *t* test, these percentages of apoptotic and necrotic cells were statistically significant in comparison to the percentages found in

siMAD2/pcDNA3.1 (22% apoptotic and 6% necrotic) and siMAD2-scramble/pcDNA3.1 (16% apoptotic and 3% necrotic) samples. In contrast, a small percentage of apoptotic cells (11% and 17%) detected in HCT116 MAD2-depleted cells and in siMAD2 scramble/pcDNA3.1-p14 cells, respectively, was not statistically significant by the Student's *t* test (Fig. 5B). The similarity between the percentage of apoptotic cells and the reduction of aneuploid cells after p14^{ARF} ectopic expression suggest apoptosis as a major mechanism to eliminate aneuploid cells (Fig. 5B). Since the p14^{ARF} gene can act in p53-dependent and p53-independent apoptotic pathways activated following DNA damage (Ozenne et al., 2010), we investigated whether p14^{ARF} cooperated with p53 activating apoptosis in response to aneuploidy. To this aim, we conducted a Western Blot analysis to evaluate the p53 protein levels. MAD2 post-transcriptional silencing and p14^{ARF} ectopic expression induced a significant increase of p53 protein levels compared to control. These findings suggest a possible collaboration between p14^{ARF} and p53 to counteract aneuploidy (Fig. 5C). To clarify the role of p53 in the induction of apoptosis after p14^{ARF} ectopic expression in aneuploid cells, we used HCT116 p53KO cells transfected with siMAD2 and pcDNA3.1-p14. The AO/EB assay in HCT116 p53KO cell, following p14^{ARF} ectopic expression showed that the percentage of apoptotic cells (20%) found in HCT116 siMAD2/pcDNA3.1-p14 cells was comparable with the percentage found in cells transfected with siMAD2 and the pcDNA3.1 empty vector (18%). Following MAD2 post-transcriptional silencing and p14^{ARF} ectopic expression, we detected the decrease of apoptotic cells in the absence of the p53 gene. This result suggests that cells were eliminated through a p53-dependent apoptotic pathway where p14^{ARF} had a key role (Fig. 6 A).

In agreement with this result cytogenetic analyses showed that siMAD2 induced higher number of aneuploid cells in HCT116 p53KO cells (61%) than siMAD2-scramble cells (21%). On the contrary, HCT116 p53KO cells that expressed p14^{ARF} ectopically showed a percentage of aneuploid cells (66%) similar to the percentage showed by HCT116 p53KO siMAD2/pcDNA3.1 cells (77%) and HCT116-siMAD2 cells (61%). These differences were not statistical significant by the Student's *t* test. Thus, in the absence of p53 activity p14^{ARF} did not induce the elimination of aneuploid cells caused by MAD2 depletion (Fig. 6B). Real Time qRT-PCR analyses confirmed

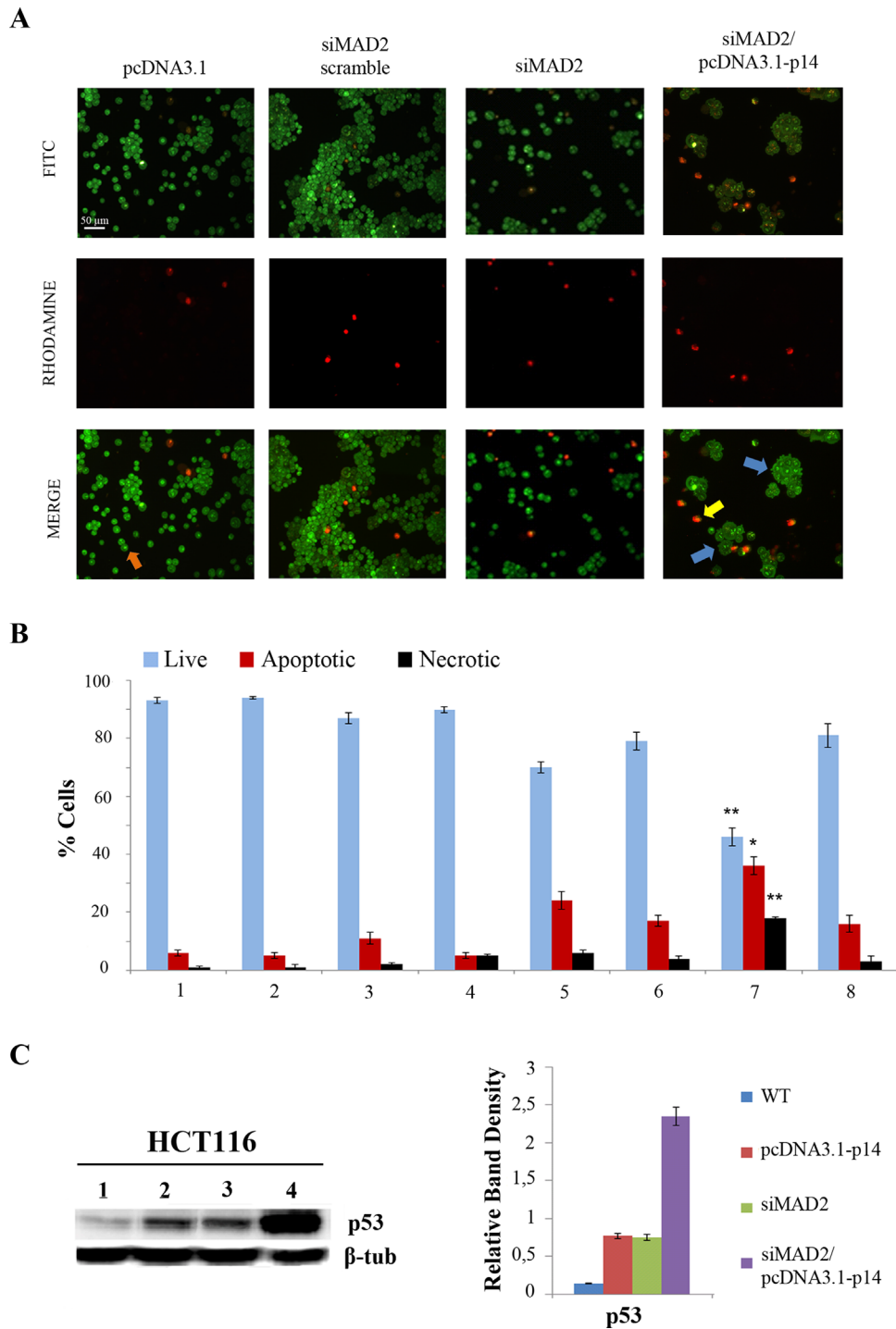


Fig. 5. p14^{ARF} ectopic expression induces apoptosis and increase of p53 protein levels in MAD2-depleted HCT116 cells. **A:** Examples of HCT116 cells stained with Orange Acridine and Ethidium Bromide 72 h after transfection; the orange arrow (merge panel, bottom left) points to live cells, yellow (white) and blue (gray) arrows point to necrotic and apoptotic cells (merge panel, bottom right), respectively. **B:** The graph summarizes the percentage of live, apoptotic and necrotic HCT116 cells transfected with pcDNA3.1 (1), pcDNA3.1-p14 (2), siMAD2 (3), siMAD2-scramble (4), siMAD2/pcDNA3.1 (5), siMAD2-scramble/pcDNA3.1-p14 (6), siMAD2/pcDNA3.1-p14 (7), and siMAD2-scramble/pcDNA3.1 (8). The experiment was repeated at least twice. (Student's *t* test * $P < 0.05$; ** $P < 0.01$, $n = 150$). **C:** Western blot analysis showing the increase of p53 protein levels after p14^{ARF} ectopic expression, in HCT116 pcDNA3.1-p14 (2), HCT116 siMAD2 (3), and in HCT116 siMAD2/pcDNA3.1-p14 (4) cells when compared to HCT116 control cells (1); on the right is showed the densitometric analysis of the WB on the left panel to quantitate the p53 protein level that is normalized to β -Tubulin.

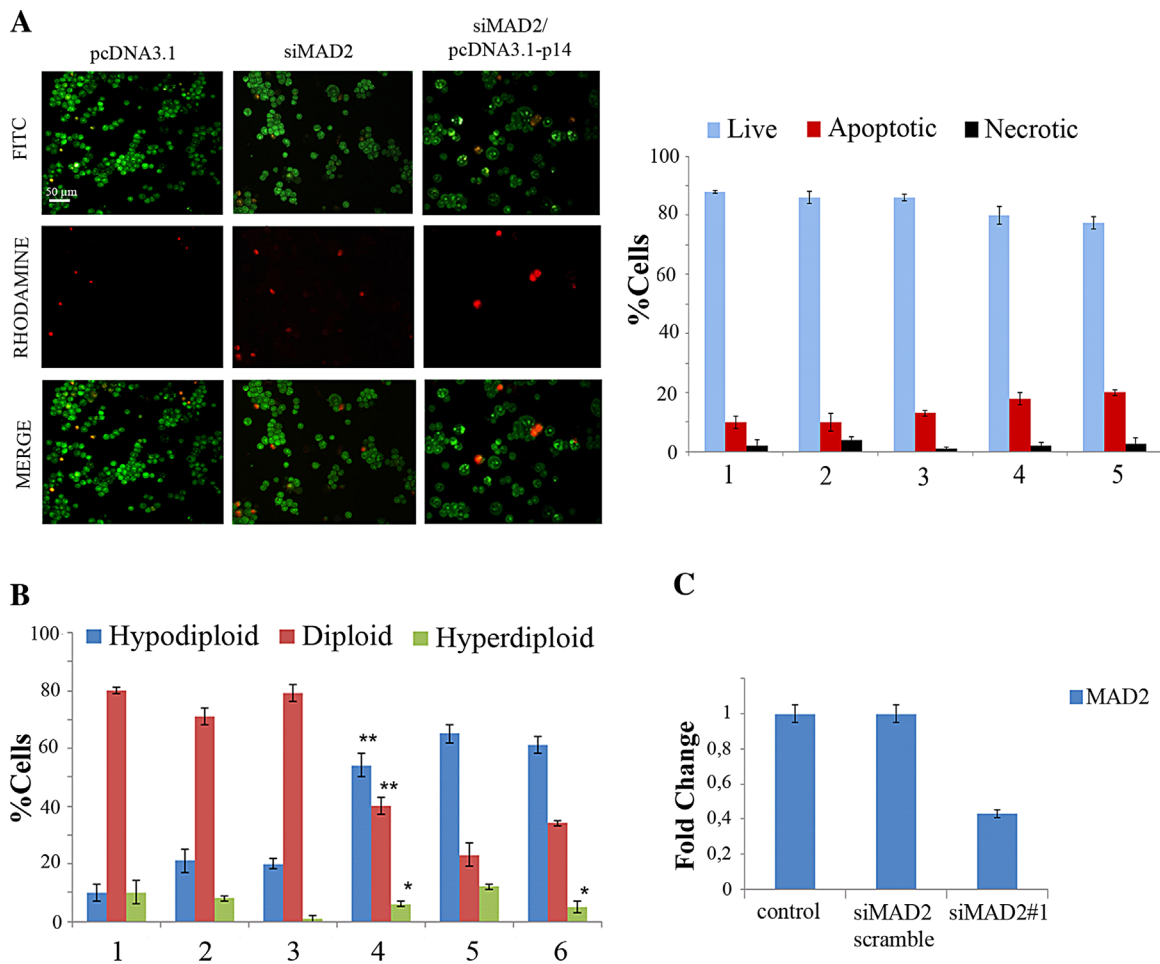


Fig. 6. p14^{ARF} does not induce apoptosis in HCT116 p53KO cells. **A:** On the left are shown representative pictures of the indicated cells stained with Orange Acridine and Ethidium Bromide solution, 72 h after transfection; the graph on the right summarizes the percentages of live, apoptotic, and necrotic cells in pcDNA3.1 (1), pcDNA3.1-p14 (2), siMAD2 (3), siMAD2/pcDNA3.1 (4), and siMAD2/pcDNA3.1-p14 (5) -HCT116 cells. **B:** The graph shows the percentages of aneuploid cells in p53 KO pcDNA3.1 (1), pcDNA3.1-p14 (2), siMAD2-scramble (3), siMAD2 (4), siMAD2/pcDNA3.1 (5), siMAD2/pcDNA3.1-p14 (6), and HCT116 cells. All experiments were repeated at least twice. (Student's *t* test * $P < 0.05$; ** $P < 0.01$, $n = 150$). **C:** Real time RT-PCR analysis showing RNA interference of siMAD2#1 and siMAD2 scramble in HCT116 p53KO cells at 72 h after transfection.

that siMAD2#1 induced MAD2 gene post-transcriptional silencing of about 50% compared to siMAD2-scramble and p53KO HCT116 cells (Fig. 6C)

Discussion

During mitosis the proper chromosomes segregation is controlled by a specific checkpoint, the Spindle Assembly Checkpoint (SAC). If any of SAC components is mutated or its expression is reduced, miss-segregation events would not be correctly reported, promoting aneuploidy development (Silva et al., 2011). The p14^{ARF} protein plays several biological functions in the cell with the purpose to suppress aberrant cell growth. The well-defined function of p14^{ARF} is to stabilize and activate p53 by neutralizing the inhibitory effects of the E3 ubiquitin ligase hMdm2 in response to oncogenic stress (hyperproliferative signals) (Sharpless, 2005). Though the p14^{ARF} protein is a key player in this p53 pathway, there are evidences that it could promote a p53-independent cell cycle

arrest and/or apoptosis (Weber et al., 2000; Muer et al., 2012). p14^{ARF} expression is generally lost by deletion or hypermethylation of CpG islands localized at its promoter region (Badal et al., 2008). Hypermethylation of p14^{ARF} promoter has been reported in many tumors, and this loss occurs at early stages of tumorigenesis in some tumors such as colorectal, gastric, prostate, and breast cancer (Ozenne et al., 2010). In many human cancers, deregulation of the p53 pathway usually occurs by inactivation of the TP53 gene through point mutations. Moreover, inactivation of the p14^{ARF} gene has been proposed as a mechanism that disrupt p53 activity in tumors with wild-type TP53 gene (Nyiraneza et al., 2012).

In agreement with our previous data (Amato et al., 2009), weakening the SAC by MAD2 post-transcriptional silencing increased aneuploidy in HCT116 cells. However, when we restored p14^{ARF} functionality by ectopic gene expression in these aneuploid cells aneuploidy, cell proliferation was reduced. At the same time, mitotic abnormality observed after MAD2 post-transcriptional silencing decreased as a result of

p14^{ARF} ectopic expression. These findings suggest that p14^{ARF} is able to prevent proliferation of aneuploid cells caused by reduction of SAC activity.

Recently, we showed (Lentini et al., 2012) that after induction of aneuploidy by MAD2 post-transcriptional silencing, human primary fibroblast activated a premature cellular senescence response p53-mediated to halt aneuploid cells proliferation. By contrast, our results show that premature cellular senescence was not activated in response to aneuploidy in HCT116 tumor cells where p14^{ARF} was ectopically expressed. The presence of apoptotic cells in MAD2-depleted HCT116 tumor cells in response to p14^{ARF} ectopic expression, suggest induction of apoptosis as the mechanism adopted by p14^{ARF} to counteract aneuploid cells proliferation. Apoptosis was associated with the increase of p53 protein, suggesting that re-expression of p14^{ARF} in these aneuploid cells induces a p53-dependent apoptosis. The existence of a p14^{ARF}-p53 axis is confirmed by experiments done in HCT116 p53KO cells, where cells interfered for MAD2 become aneuploidy but did not show increased number of apoptotic cells when p14^{ARF} was re-expressed.

Previously, it was suggested that a p38 kinase-dependent stress response activates p53 to induce the p21^{waf1} in response to chromosome mis-segregation in HCT116 cells (Thompson and Compton, 2010). Likely, the cellular signal triggering this pathway relies on the presence of DNA damage that could be caused by chromosomal mechanical stress. On the contrary, our results suggest that, after p14^{ARF} re-expression, apoptosis activation p53-dependent hampers aneuploid cell proliferation. Most likely, this mechanism could signal the presence of gene expression imbalance resulting from chromosome mis-segregation (Williams et al., 2008). Generally, gene expression correlates with gene copy number and aneuploidy, then unbalancing genomic material could induce a signal resembling hyperproliferative signals that are typically sensed by p14^{ARF}.

Finally, our findings reinforce the idea that the abolition of p14^{ARF} expression or p14^{ARF} related partners that control genomic stability is one of the strategies adopted by human tumor cells to tolerate aneuploidy.

Acknowledgments

We thank Prof. Silvye Gazzeri, University J. Fourier - La Tronche – France, for providing us with the pcDNA3.1 p14 plasmid. This work was partly supported by a grant from University of Palermo to ADL (FFR 2012-13, ATE-0255).

Literature Cited

- Amato A, Lentini L, Schillaci T, Iovino F, Di Leonardo A. 2009. RNAi mediated acute depletion of retinoblastoma protein (pRb) promotes aneuploidy in human primary cells via micronuclei formation. *BMC Cell Biol* 10:79.
- Ayrault O, Andrieu L, Fauvin D, Eymin B, Gazzeri S, Seité P. 2006. Human tumor suppressor p14ARF negatively regulates rRNA transcription and inhibits UBF1 transcription factor phosphorylation. *Oncogene* 25:7577–7586.
- Badal V, Menendez S, Coomber D, Lane D P. 2008. Regulation of the p14ARF promoter by DNA methylation. *Cell Cycle* 7:112–119.
- Barra V, Schillaci T, Lentini L, Costa G, Di Leonardo A. 2012. Bypass of cell cycle arrest induced by transient DNMT1 post-transcriptional silencing triggers aneuploidy in human cells. *Cell Div* 7:2.
- Burri N, Shaw P, Bouzourene H, Sordat I, Sordat B, Gillet M, Schorderet D, Bosman FT, Chaubert P. 2001. Methylation silencing and mutations of the p14ARF and p16INK4a genes in colon cancer. *Lab Invest* 81:217–229.
- Hanks S, Coleman K, Reid S, Plaja A, Firth H, FitzPatrick D, Kidd A, Méhes K, Nash R, Robin N, Shannon N, Tolmie J, Swansbury J, Irrthum A, Douglas J, Rahman N. 2004. Constitutional aneuploidy and cancer predisposition caused by allelic mutations in BUB1B. *Nat Genet* 36:1159–1161.
- Holland AJ, Cleveland DW. 2009. Boveri revisited: chromosomal instability, aneuploidy and tumorigenesis. *Nat Rev Mol Cell Biol* 10:478–487.
- Lengauer C, Kinzler KW, Vogelstein B. 1997. Genetic instability in colorectal cancers. *Nature* 386:623–627.
- Lentini L, Barra V, Schillaci T, Di Leonardo A. 2012. MAD2 depletion triggers premature cellular senescence in human primary fibroblasts by activating a p53 pathway preventing aneuploid cells propagation. *J Cell Physiol* 227:3324–3332.
- Michel LS, Liberal V, Chatterjee A, Kirchwegger R, Pasche B, Gerald W, Dobles M, Sorger PK, Murty VV, Benzra R. 2001. MAD2 haplo-insufficiency causes premature anaphase and chromosome instability in mammalian cells. *Nature* 409:355–359.
- Müer A, Overkamp T, Gillissen B, Richter A, Pretzsch T, Milojkovic A, Dörken B, Daniel PT, Hemmati P. 2012. p14(ARF)-induced apoptosis in p53 protein-deficient cells is mediated by BH3-only protein-independent derepression of Bak protein through down-regulation of Mcl-1 and Bcl-xL proteins. *J Biol Chem* 287:17343–17352.
- Nyiraneza C, Sempoux C, Detry R, Kartheiser A, Dahan K. 2012. Hypermethylation of the 5' CpG island of the p14ARF flanking exon 1 beta in human colorectal cancer displaying a restricted pattern of p53 overexpression concomitant with increased MDM2 expression. *Clin Epigenetics* 4:9.
- Ozanne P, Eymin B, Brambilla E, Gazzeri S. 2010. The ARF tumor suppressor: Structure, functions and status in cancer. *International journal of cancer. Int J Cancer* 127:2239–2247.
- Sharpless NE. 2005. INK4a/ARF: A multifunctional tumor suppressor locus. *Mutat Res* 576:22–38.
- Silk AD, Zasadile LM, Holland AJ, Vitre B, Cleveland DW, Weaver BA. 2013. Chromosome missegregation rate predicts whether aneuploidy will promote or suppress tumors. *Proc Natl Acad Sci USA* 110:E4134–E4141.
- Silva P, Barbosa J, Nascimento AV, Faria J, Reis R, Bousbaa H. 2011. Monitoring the fidelity of mitotic chromosome segregation by the spindle assembly checkpoint. *Cell Prolif* 44:391–400.
- Sussan TE, Yang A, Li F. 2008. Trisomy represses Apc^(Min)-Mediated tumours in mouse models of Down's syndrome. *Nature* 451:73–75.
- Thompson SL, Compton DA. 2010. Proliferation of aneuploid human cells is limited by a p53-dependent mechanism. *J Cell Biol* 188:369–381.
- Thompson SL, Compton DA. 2011. Chromosome missegregation in human cells arises through specific types of kinetochore-microtubule attachment errors. *Proc Natl Acad Sci USA* 108:17974–17978.
- Weaver BA, Cleveland DW. 2007. Aneuploidy: Instigator and inhibitor of tumorigenesis. *Cancer Res* 67:10103–10105.
- Weaver BA, Cleveland DW. 2009. The role of aneuploidy in promoting and suppressing tumors. *J Cell Biol* 185:935–937.
- Weaver BA, Silk AD, Montagna C. 2007. Aneuploidy acts both oncogenically and as a tumor suppressor. *Cancer Cell* 11:25–36.
- Weber JD, Jeffers JR, Reh JE, Randle DH, Lozano G, Roussel MF, Sherr CJ, Zambetti GP. 2000. P53-independent functions of the p19(ARF) tumor suppressor. *Genes Dev* 14:2358–2365.
- Williams BR, Prabhu VR, Hunter KE, Glazier CM, Whittaker CA, Housman DE, Amon A. 2008. Aneuploidy affects proliferation and spontaneous immortalization in mammalian cells. *Science* 322:703–709.